



# CHORUS

This is the accepted manuscript made available via CHORUS. The article has been published as:

## Swimming of a model ciliate near an air-liquid interface

S. Wang and A. M. Ardekani

Phys. Rev. E **87**, 063010 — Published 17 June 2013

DOI: [10.1103/PhysRevE.87.063010](https://doi.org/10.1103/PhysRevE.87.063010)

# Swimming of a model ciliate near an air-liquid interface

S. Wang and A. M. Ardekani

*Aerospace and Mechanical Engineering,*

*University of Notre Dame, Notre Dame, IN 46556, USA*

(Dated: May 13, 2013)

## Abstract

In this work, the role of the hydrodynamic forces on a swimming microorganism near an air-liquid interface is studied. The lubrication theory is utilized to analyze hydrodynamic effects within the narrow gap between a flat interface and a small swimmer. By using an archetypal low-Reynolds-number swimming model called “squirmers”, we find that the magnitude of the vertical swimming velocity is in the order of  $O(\epsilon \log \epsilon)$ , where  $\epsilon$  is the ratio of the gap width to the swimmer’s body size. The reduced swimming velocity near an interface can explain experimental observations of the aggregation of microorganisms near a liquid interface.

## I. INTRODUCTION

Low-Reynolds-number swimming near an air-liquid interface has inspired several interesting works in the recent years [1–4]. This configuration has been used to devise “soft swimming” [1] which employs the deformation of a free surface to generate either parallel or perpendicular locomotion relative to the interface even under reciprocal movement, thus surmounting the constraint of the scallop theorem. In the so-called “bacterial driven micromotor” [2], a micron-size gear, immersed in an active bacterial bath, is located at an air-liquid interface to reduce friction. Besides engineering applications, the interaction between microorganisms and the air-liquid interface is also frequently encountered in nature. For example, the sea surface microlayer, which is the uppermost tens to hundreds of  $\mu\text{m}$  of the surface of the ocean, contains a large population of microorganisms in marine environments [3]. The organisms inhabiting the sea surface microlayer are called “neuston” [5], e.g. bacterioneuston, phytoneuston and zooneuston [3]. The physicochemical properties of the air-water interface as a habitat for microorganisms have been extensively studied [6], however, the hydrodynamic effects of the interface on the locomotion of microorganisms is poorly understood. Di Leonardo *et al.* have recently shown that *E. coli* bacteria exhibit anticlockwise oriented circular trajectories near an air-liquid interface. They have considered the hydrodynamic coupling of the bacterium and its mirror image to satisfy the “perfect-slip” boundary condition at the interface [4]. More recently, Ferracci *et al.* have shown that *Tetrahymena*, fresh-water ciliate protozoa, can be trapped at an air-water interface [7] and form large aggregates. By excluding the potential effects of chemotaxis and gravitaxis, the entrapment was found to be due to hydrodynamic effects. The present paper utilizes lubrication theory for an archetypal low-Reynolds-number swimming model “squirmers” to describe the hydrodynamic effects leading to the entrapment of ciliates near an air-liquid interface.

A superposition of point force singularities can be used to describe the far field solution of particles or microorganisms near an interface or a solid surface [8, 9]. The numerical solution for the motion of a rigid particle shows that this method provides a good approximation when the distance between the particle and the interface is more than 2.5 times particle radius [9]. Point force singularities combined with Faxén law are also used to study bacteria swimming near a rigid wall [8]. Even though point force singularities capture the far

field solution of swimming bacteria near a rigid wall, including wall-induced attraction and pitching dynamics, the wall effect cannot be accurately captured if the separation distance is smaller than the microorganism's body size [8]. Here, we utilize the lubrication theory in order to capture the low-Reynolds-number swimming of a ciliate near an air-liquid interface for  $\epsilon \ll 1$ , where  $\epsilon$  is the ratio of the gap width between the swimmer's surface and the interface to the swimmer's body size.

Let us describe the profile of the air-liquid interface as  $S = z - f(\varrho, \phi, \tau)$ , where  $(\varrho, \phi, z)$  are the dimensionless cylindrical coordinates and  $\tau$  is the dimensionless time, which are scaled by characteristic length,  $a$  (size of the swimmer) and time,  $a/U$ , respectively. Characteristic velocity  $U$  is the swimming velocity of the swimmer in an unbounded fluid domain. The kinematic and dynamic boundary conditions of the interface under negligible gravitational effects can be written as

$$\frac{DS}{D\tau} = -\frac{\partial f}{\partial \tau} + \frac{1}{\kappa} \mathbf{n} \cdot \mathbf{u} = 0, \quad (1)$$

$$-Ca(\mathbf{n} \cdot \boldsymbol{\sigma}) = \mathbf{n}(\nabla \cdot \mathbf{n}) - \nabla \gamma, \quad (2)$$

where  $D/D\tau$  denotes the material time derivative,  $\mathbf{n} = \nabla S / \|\nabla S\|$  is the unit direction vector normal to the interface and  $\kappa = 1/\|\nabla S\|$  is the local curvature,  $\mathbf{u}$  is the dimensionless velocity field, and  $\boldsymbol{\sigma}$  is the dimensionless stress tensor. The characteristic stress tensor is  $\mu U/a$ , where  $\mu$  is fluid viscosity. Hereafter unless otherwise stated, the variables are written in the dimensionless form. The dimensionless surface tension,  $\gamma$ , can be nonuniform if surfactants are present. The capillary number,  $Ca = \mu U/\gamma_s$ , is defined as the ratio of the viscous force to the surface tension force, where  $\mu$  is the fluid viscosity,  $\gamma_s$  is the interfacial tension of the clean fluid interface, and  $U$  is the swimming velocity in an unbounded fluid domain. For microorganisms in an aquatic environment,  $Ca$  is generally small: for *Opalina*,  $Ca \sim 10^{-6}$  and for *Paramecium*,  $Ca \sim 10^{-5}$ . Therefore, in the case of constant surface tension, a perturbation in terms of  $Ca$  results in a leading order boundary condition of  $\mathbf{n} \cdot \mathbf{u}^{(0)} = 0$  and  $\mathbf{t} \cdot \mathbf{n} \cdot \boldsymbol{\sigma}^{(0)} = 0$ , where  $\mathbf{t}$  is the unit tangential vector. The leading order boundary condition basically corresponds to a flat interface and is referred to as a ‘‘perfect-slip’’ boundary condition. In order to explore the hydrodynamic mechanism behind the entrapment of microorganisms near an air-liquid interface, we use a squirmer model [10] which consists of a spherical cell that swims using wavelike deformations of its surface [11], approximating ciliates moving by synchronized beating of cilia on their surface [10] or using

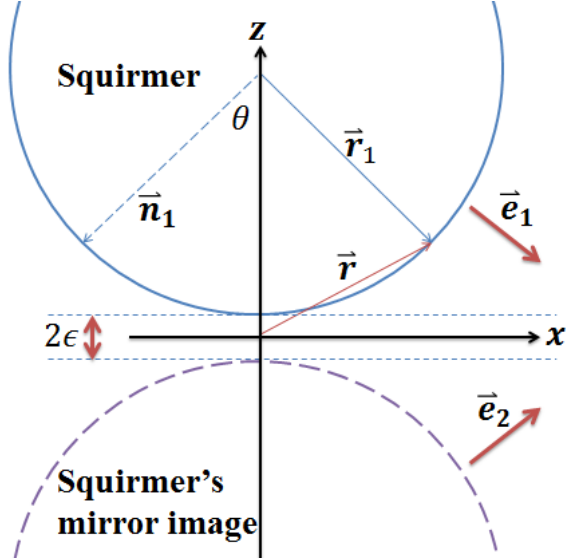


FIG. 1. Schematic of a squirmer and its mirror image

colonies of flagellates such as Volvox [12].

## II. MATHEMATICAL MODEL

In the low Reynolds number regime, the pressure and the flow field satisfy the Stokes equation. We write the governing equations in the dimensionless form,

$$-\nabla p + \nabla^2 \mathbf{u} = 0, \quad (3)$$

$$\nabla \cdot \mathbf{u} = 0, \quad (4)$$

where  $p$  is the pressure. Di Leonardo *et al.* considered a mirror image at the opposite side of the interface to satisfy the “perfect-slip” condition in the case of swimming *E. coli* near a free surface [4]. The so called “perfect-slip” condition requires zero velocity in  $z$  direction and zero tangential shear stress on the interface. These conditions can be satisfied by adding a mirror image of the squirmer on the opposite side of the interface, where the mirror image has the same speed as the real squirmer, but its direction of rotation and translation along the vertical direction are opposite of the real squirmer. Therefore, the problem of swimming near a flat interface is analogous to two squirmers generating symmetric surface motion relative to the interface. As shown in Fig. 1, the  $z = 0$  plane is the interface and we assume the squirmer is located in the  $z > 0$  region while its mirror image is in the  $z < 0$  region.

The surfaces of the two spherical squirmers in the narrow gap region can be approximated as two parabolic surfaces

$$\begin{aligned} h_1 &= \left( \epsilon + \frac{\varrho^2}{2} + \dots \right), \\ h_2 &= - \left( \epsilon + \frac{\varrho^2}{2} + \dots \right), \end{aligned} \quad (5)$$

where  $\varrho$  is the dimensionless radius in the cylindrical coordinate with its origin at the midpoint between the two squirmers. The stretched coordinates  $(X, Y, Z)$ , widely used in the lubrication theory of nearly touching spheres, are defined as

$$\begin{aligned} \epsilon^{1/2} X &= x, \epsilon^{1/2} Y = y, (\varrho = \sqrt{x^2 + y^2}, \epsilon^{1/2} \rho = \varrho), \\ \epsilon Z &= z. \end{aligned} \quad (6)$$

where  $(x, y, z)$  are the cartesian coordinates with an origin at the midpoint between two squirmers and  $\rho = \sqrt{X^2 + Y^2}$ , is the stretched radius in the cylindrical coordinate. The surface of both squirmers,  $h_1$  and  $h_2$ , can be simplified using the above stretched coordinates as  $H_1 = h_1/\epsilon = 1 + \rho^2/2, H_2 = -H_1$ . The governing equations (3)-(4) are rewritten using the stretched coordinates  $(X, Y, Z)$  as

$$\left( \epsilon \left( \frac{\partial^2}{\partial X^2} + \frac{\partial^2}{\partial Y^2} \right) + \frac{\partial^2}{\partial Z^2} \right) \mathbf{u} = \epsilon \left( \epsilon^{1/2} \frac{\partial p}{\partial X}, \epsilon^{1/2} \frac{\partial p}{\partial Y}, \frac{\partial p}{\partial Z} \right), \quad (7)$$

$$\epsilon^{1/2} \left( \frac{\partial u}{\partial X} + \frac{\partial v}{\partial Y} \right) + \frac{\partial w}{\partial Z} = 0. \quad (8)$$

Here, we neglect small radial displacements of cilia and following Blake [10], we impose a tangential velocity,  $\mathbf{u}_s$ , on the swimmer's surface

$$\mathbf{u}_s = ((\mathbf{e}_1 \cdot \mathbf{r}_1) \mathbf{r}_1 - \mathbf{e}_1) \sum_{n=1}^{\infty} B_n W_n(\mathbf{e}_1 \cdot \mathbf{r}_1), \quad (9)$$

where  $B_n$  is dimensionless constant.  $W_n(\eta) = \frac{2}{n(n+1)} \frac{dP_n}{d\eta}$ , where  $P_n$  is the Legendre polynomial of the first kind of degree  $n$ .  $\mathbf{e}_1$  describes the swimming direction of the squirmer while  $\mathbf{e}_2$  is along the swimming direction of the squirmer's mirror image.  $\mathbf{e}_1 = e_{11} \mathbf{e}_x + e_{13} \mathbf{e}_z$ , where  $e_{11}^2 + e_{13}^2 = 1$ . As shown in Fig. 1,  $\mathbf{r}_1 = \mathbf{r} - (1 + \epsilon) \mathbf{e}_z$  is a position vector describing the surface of the squirmer whose origin is located at the center of the squirmer whereas  $\mathbf{r}$  is a position vector measured from the origin of the cylindrical coordinate (midpoint between the

two squirmers). Following the procedure given by Ishikawa *et al.* [13], Eq. (9) is expanded in terms of  $\epsilon^{1/2}$  as

$$\mathbf{u}_s = \mathbf{u}_s^{(0)} + \epsilon^{1/2}\mathbf{u}_s^{(1)} + O(\epsilon), \quad (10)$$

where

$$\mathbf{u}_s^{(0)} = ((\mathbf{e}_1 \cdot \mathbf{e}_z)\mathbf{e}_z - \mathbf{e}_1) \sum_{n=1}^{\infty} B_n W_n(-\mathbf{e}_1 \cdot \mathbf{e}_z), \quad (11)$$

$$\begin{aligned} \mathbf{u}_s^{(1)} = & (\mathbf{e}_1 \cdot \boldsymbol{\rho})((\mathbf{e}_1 \cdot \mathbf{e}_z)\mathbf{e}_z - \mathbf{e}_1) \sum_{n=1}^{\infty} B_n W'_n(-\mathbf{e}_1 \cdot \mathbf{e}_z) \\ & - ((\mathbf{e}_1 \cdot \boldsymbol{\rho})\mathbf{e}_z + (\mathbf{e}_1 \cdot \mathbf{e}_z)\boldsymbol{\rho}) \sum_{n=1}^{\infty} B_n W_n(-\mathbf{e}_1 \cdot \mathbf{e}_z), \end{aligned} \quad (12)$$

where  $\boldsymbol{\rho} = \rho \mathbf{e}_\rho$ ,  $\mathbf{e}_\rho$  is the unit radial vector in the cylindrical coordinate, and  $W'_n = \frac{dW_n}{d\eta}$ . It is found that  $\mathbf{u}_s^{(0)}$  provides a uniform velocity condition while  $\mathbf{u}_s^{(1)}$  is a linear function of position,  $\boldsymbol{\rho}$ . Similarly the velocity components  $(u, v, w)$  and the pressure field are perturbed in terms of  $\epsilon^{1/2}$ :

$$\begin{aligned} u &= u_0 + \epsilon^{1/2}u_1 + \dots, \\ v &= v_0 + \epsilon^{1/2}v_1 + \dots, \\ w &= \epsilon^{1/2}(w_0 + \epsilon^{1/2}w_1 + \dots), \\ p &= p_\infty + \epsilon^{-3/2}(p_0 + \epsilon^{1/2}p_1 + \dots), \end{aligned} \quad (13)$$

where  $p_\infty$  is the reference pressure at the outermost point of the thin lubrication region.

We follow a two-step procedure in order to determine the translational velocity,  $\mathbf{U}$ , and angular velocity,  $\boldsymbol{\Omega}$ , of the squirmer [13]: first we calculate the force and torque due to the squirming motion,  $\mathbf{u}_s$ , generated by a fixed squirmer; in the next step, the translational and angular velocity of the squirmer due to the calculated force and torque will be determined. The governing equations for the leading order solution can be obtained by substituting Eqs. (13) into Eq. (7):

$$\begin{aligned} \frac{\partial^2 u_0}{\partial Z^2} &= \frac{\partial p_0}{\partial X}, \\ \frac{\partial^2 v_0}{\partial Z^2} &= \frac{\partial p_0}{\partial Y}, \\ \frac{\partial p_0}{\partial Z} &= 0. \end{aligned} \quad (14)$$

The leading order solution of Eq. (14) is a uniform flow field independent of position

$$\begin{aligned} u_0 &= \mathbf{u}_s^{(0)} \cdot \mathbf{e}_x, & v_0 &= \mathbf{u}_s^{(0)} \cdot \mathbf{e}_y, \\ w_0 &= \mathbf{u}_s^{(0)} \cdot \mathbf{e}_z = 0. \end{aligned} \quad (15)$$

Therefore, the solution to this order provides null pressure ( $p_0 = 0$ ) in the lubrication region. There is no force or torque acting on the squirmer at the zeroth order. The governing equations of the next order are identical to the zeroth order, however, the boundary condition is different since  $\mathbf{u}_s^{(1)}$  provides nonzero vertical velocity ( $\mathbf{u}_s^{(1)} \cdot \mathbf{e}_z$ ) and horizontal velocities ( $\mathbf{u}_s^{(1)} \cdot \mathbf{e}_x$  and  $\mathbf{u}_s^{(1)} \cdot \mathbf{e}_y$ ),

$$\begin{aligned} \mathbf{u}_s^{(1)} \cdot \mathbf{e}_x &= - \left( e_{11}^2 \sum_{n=1}^{\infty} B_n W_n' + e_{13} \sum_{n=1}^{\infty} B_n W_n \right) X, \\ \mathbf{u}_s^{(1)} \cdot \mathbf{e}_y &= - \left( e_{13} \sum_{n=1}^{\infty} B_n W_n \right) Y, \\ \mathbf{u}_s^{(1)} \cdot \mathbf{e}_z &= \left( - \sum_{n=1}^{\infty} B_n W_n \right) \rho(\mathbf{e}_1 \cdot \mathbf{e}_\rho). \end{aligned} \quad (16)$$

The pressure at this order,  $p_1(X, Y)$ , is not a function of the vertical position  $Z$ . Consequently, momentum equations along  $X$  and  $Y$  directions give

$$\begin{aligned} u_1 &= \frac{1}{2} \frac{\partial p_1}{\partial X} (Z^2 - H_1^2) + \mathbf{u}_s^{(1)} \cdot \mathbf{e}_x, \\ v_1 &= \frac{1}{2} \frac{\partial p_1}{\partial Y} (Z^2 - H_1^2) + \mathbf{u}_s^{(1)} \cdot \mathbf{e}_y. \end{aligned} \quad (17)$$

In order to determine the pressure field,  $p_1$ , we use the incompressibility condition combined with the boundary condition on the squirmer's surface:

$$\begin{aligned} \int_{-H_1}^{H_1} \frac{\partial w_1}{\partial Z} dZ &= \frac{2}{3} H_1^3 \left( \frac{\partial^2 p_1}{\partial X^2} + \frac{\partial^2 p_1}{\partial Y^2} \right) \\ &\quad + 2H_1^2 \left( X \frac{\partial p_1}{\partial X} + Y \frac{\partial p_1}{\partial Y} \right) + 4CH_1, \end{aligned} \quad (18)$$

where  $w_1(H_1) = -w_1(-H_1) = \mathbf{u}_s^{(1)} \cdot \mathbf{e}_z = (-\sum_{n=1}^{\infty} B_n W_n) \rho(\mathbf{e}_1 \cdot \mathbf{e}_\rho)$  and  $C = (e_{11}^2/2) \sum_{n=1}^{\infty} B_n W_n' + e_{13} \sum_{n=1}^{\infty} B_n W_n$ . Consequently, the governing equation for the pressure,  $p_1$ , can be derived as:

$$\frac{2}{3} H_1^3 \nabla_{\perp}^2 p_1 + 2H_1^2 (\boldsymbol{\rho} \cdot \nabla_{\perp} p_1) + 4CH_1 = 2B\rho(\mathbf{e}_1 \cdot \mathbf{e}_\rho), \quad (19)$$

where  $B = -\sum_{n=1}^{\infty} B_n W_n$  and  $\nabla_{\perp} = \left( \frac{\partial}{\partial X}, \frac{\partial}{\partial Y}, 0 \right)$ . Since pressure can be written as  $p_1 = p_a + (\mathbf{e}_1 \cdot \mathbf{e}_\rho) p_s$ , Eq. (19) can be decomposed as:

$$\frac{H_1^3}{3\rho} \frac{\partial}{\partial \rho} \left( \rho \frac{\partial p_a}{\partial \rho} \right) + H_1^2 \left( \rho \frac{\partial p_a}{\partial \rho} \right) + 2CH_1 = 0,$$

$$\frac{H_1^3}{3\rho} \frac{\partial}{\partial \rho} \left( \rho \frac{\partial p_s}{\partial \rho} \right) - \frac{H_1^3}{3} \frac{p_s}{\rho^2} + H_1^2 \left( \rho \frac{\partial p_s}{\partial \rho} \right) = B\rho. \quad (20)$$

The solution to these equations are:

$$p_a = C \left( \frac{3}{2H_1} + \frac{3}{4H_1^2} \right), \quad (21)$$

$$p_s = -\frac{3B\rho}{5H_1^2}. \quad (22)$$

The pressure field for a swimmer near a flat interface and a rigid wall are dramatically different; the first non-zero term for the latter case is of order  $O(\epsilon^{-3/2})$  instead of  $O(\epsilon^{-1})$ . In other words, the pressure of a ciliate swimming near an interface is an order of magnitude lower than near a rigid wall. Having the pressure field  $p_1$ , the flow field in the cylindrical coordinate can be written as:

$$\begin{aligned} u_{\rho,1} &= \mathbf{e}_\rho \cdot \left( \nabla p_1 \frac{Z^2 - H_1^2}{2} + \mathbf{u}_s^{(1)} \right), \\ u_{\phi,1} &= \mathbf{e}_\phi \cdot \left( \nabla p_1 \frac{Z^2 - H_1^2}{2} + \mathbf{u}_s^{(1)} \right). \end{aligned} \quad (23)$$

The vertical component of the velocity field  $u_{z,1}$  can be calculated using the incompressibility condition. The details of these velocity components are provided in the Appendix. Next, we evaluate the force acting on the squirmer,  $F_z$ . The force element  $dF_z$  acting on the element of surface area of the squirmer  $dA$  is given as

$$\begin{aligned} dF_z &= \mathbf{e}_z \cdot (\boldsymbol{\sigma} \cdot \mathbf{n}_1) dA \\ &= [-p(\mathbf{e}_z \cdot \mathbf{n}_1) + 2(\mathbf{e}_\rho \cdot \mathbf{n}_1)E_{\rho z} + 2(\mathbf{e}_z \cdot \mathbf{n}_1)E_{zz}] dA, \end{aligned} \quad (24)$$

where  $\mathbf{n}_1 = -\cos\theta\mathbf{e}_z + \sin\theta\mathbf{e}_\rho$  and  $\theta$  is the polar angle shown in Fig. 1, and  $\mathbf{E} = (\nabla\mathbf{u} + \nabla\mathbf{u}^T)/2$  is the strain rate tensor. The force  $F_z$  is evaluated on the surface of the squirmer ( $Z = H_1$ ). In the gap region,  $\epsilon^{1/2}\rho = \sin\theta$  and  $d\rho = \epsilon^{-1/2}\sqrt{1-\epsilon\rho^2}d\theta$ . The contribution of shear stress to the force acting on the squirmer is much smaller than the contribution of pressure. Therefore,

$$F_z \sim 3\pi C \int_\theta \frac{\epsilon^{-1}}{H_1} \cos\theta \sin\theta d\theta = 3\pi C \int_0^{\rho_0} \frac{\rho}{H_1} d\rho \sim 3C\pi \log \rho_0^2, \quad (25)$$

where  $\rho_0$  is the radius below which the lubrication theory is valid.  $\rho_0$  is of order  $\rho_0 \sim D/\epsilon^{1/2}$ , where  $D \sim O(1)$ . Consequently, the vertical force can be written as

$$F_z = 3C\pi (-\log \epsilon + O(1)), \quad (26)$$

where the leading order force is independent of the exact value of  $\rho_0$ . The result is consistent with the numerical prediction of Ishikawa *et al.* [13]. The  $O(1)$  constant can be calculated by matching the lubrication solution with the solution outside the gap region similar to the calculation of Jeffery and Corless [14] for a rigid sphere. However, this step is not done here, since the focus of this paper is on the leading order effect of the interface on the biolocomotion, where  $\epsilon \ll 1$ . For a moderately small  $\epsilon$ , the  $O(1)$  constant cannot be neglected and can be calculated numerically [13], which is outside the scope of the present manuscript.

In order to calculate the swimming velocity of the squirmer, the solution for the squeezing motion of two spherical rigid particles is required. A sphere moving towards a fixed sphere with constant dimensionless velocity,  $U$ , will experience a dimensionless force  $F \sim -6\pi/8\epsilon$  [15]. This is equivalent of having two spheres moving toward each other with half that velocity,  $U/2$ . Therefore, the squirmer's velocity perpendicular to the interface is estimated as

$$U_z \sim \left( e_{11}^2 \sum_{n=1}^{\infty} B_n W_n' + 2e_{13} \sum_{n=1}^{\infty} B_n W_n \right) \epsilon \log \epsilon. \quad (27)$$

The contribution of the pressure force to the horizontal component of the force,  $F_x$ , and torque  $T_y$  is the same order as the contribution of the shear stress to the force and torque. Therefore, their leading effects are in the order of  $O(\epsilon^{1/2} \log \epsilon)$  (see Appendix) which does not provide a singular term in the lubrication region and is zero as  $\epsilon \rightarrow 0$ . This is equivalent to saying that the small gap does not have a dominant effect on the horizontal swimming and pitching behavior of the squirmer.

So far, we have focused on the motion of a squirmer near an air-liquid interface utilizing a lubrication theory. The far field effect of the interface on the linear and angular velocity of the squirmer does not follow the discussion above and it has been previously discussed by Spagnolie and Lauga [8] and is summarized here. The far field solution of a squirmer in an unbounded domain with  $B_n = 0$  for  $n > 2$  can be approximated by the superposition of a force dipole (Stresslet,  $\sim O(R^{-2})$ ), potential dipole ( $\sim O(R^{-3})$ ), and potential quadrupole ( $\sim O(R^{-4})$ ) [16], where  $R$  is the dimensionless distance between a point in the domain and the center of the squirmer. The leading order velocity field can be approximated as a force dipole  $\mathbf{D}_1 = \frac{\beta}{R^3} \left( 1 - 3 \frac{(\mathbf{e}_1 \cdot \mathbf{R})^2}{R^2} \right)$  [17], where  $\beta = B_2/B_1$ . Different signs of  $\beta$  describes two different types of swimmers.  $\beta < 0$  represents the case where the thrust is generated behind

the swimmer, called a pusher.  $\beta > 0$  describes a swimmer that generates thrust in front of its body, called a puller. In order to consider the effect of the interface, the flow field generated by the dipole's mirror image,  $\mathbf{D}_2$ , should be included as well. For a force-free and torque-free swimmer, the free surface induces a vertical velocity  $U_z$  and angular velocity  $\Omega_y$  on the swimmer that are given as [8]

$$U_z = \frac{\beta(1 - 3e_{13}^2)}{8d^2}, \quad \Omega_y = \frac{3\beta e_{11}e_{13}}{8d^2}, \quad (28)$$

where  $d$  is the dimensionless distant between the center of the squirmer and the interface. A pusher near an interface rotates until its orientation is parallel to the interface. In this case, there exist an attractive force between the swimmer and the interface. For a swimmer with an orientation  $e_{11}/e_{13} < \sqrt{2}$ , there is a repulsive force between the swimmer and the interface, however, the hydrodynamic torque leads to the reorientation of the swimmer until it is parallel to the interface. A puller will rotate in the opposite direction and its equilibrium orientation is perpendicular to the interface. Consequently, the far field solution leads to the attraction of a swimmer towards the interface independent of the swimming type.

### III. DEFORMABILITY OF AIR-LIQUID INTERFACE

The discussion above is valid for a flat interface. Here, we estimate the deformability of the interface due to the motion of the swimmer. For a clean interface, the stress condition Eq. (2) along the direction normal to the interface is written as  $\sigma_{zz} = -(1/Ca)\nabla \cdot \mathbf{n}$ . The dimensionless deformation of the interface,  $\delta$ , is estimated by the balance of viscous and surface tension forces. For  $\epsilon \sim O(1)$ ,  $\delta \sim \mu U/\gamma_s (= Ca)$ . For  $\epsilon \ll 1$ , the stress  $\sigma_{zz}$  can be written as

$$\begin{aligned} \sigma_{zz} = C & \left( -\frac{3}{2\epsilon H_1} - \frac{3}{4\epsilon H_1^2} - 2 + \frac{3\rho^2}{2H_1} + \frac{3\rho^2}{2H_1^2} \right) \\ & + B(\mathbf{e}_1 \cdot \mathbf{e}_\rho) \left( \frac{3\rho}{5\epsilon H_1^2} + \frac{18\rho}{5H_1} - \frac{6\rho^3}{5H_1^2} \right), \end{aligned} \quad (29)$$

and is of order  $O(\epsilon^{-1})$ . Therefore, the deformation of the interface is of order  $\delta/\epsilon \sim \epsilon^{-2}Ca$ . For *Tetrahymena* in fresh water,  $Ca \sim O(10^{-5})(U \sim 700 \mu\text{m/s}, \mu \sim 10^{-3} \text{ Pa}\cdot\text{s}, \gamma_s \sim 0.07 \text{ N/m})$  [7]. Consequently, the deformation is negligible even for a gap equal to one tenth of the swimmer's body size ( $\epsilon \sim 0.1$ ).

#### IV. ROLE OF SURFACTANTS

Next, we evaluate the role of surfactants on the interface and the swimming behavior of ciliates near an air-liquid interface. A considerable concentration of surface active dissolved organic agents (surfactants) are found in the sea surface microlayer [18]. The tangential interfacial stress condition, Eq. (2), can be rewritten as

$$Ca(\mathbf{t}\cdot\mathbf{n}\cdot\boldsymbol{\sigma}) - \mathbf{t}\cdot\nabla\gamma = 0. \quad (30)$$

For a flat interface, Eq. (30) is simplified as

$$\mathbf{t}\cdot\mathbf{n}\cdot\boldsymbol{\sigma} = \frac{1}{\epsilon^{1/2}Ca} \frac{\partial\gamma}{\partial\rho}. \quad (31)$$

Eq. (31) is derived for the axisymmetric case ( $\gamma = \gamma(\rho)$ ), when the swimmer swims perpendicular to the interface. The surface tension is related to the concentration of surfactants at the interface  $\Gamma$  by means of the Langmuir limit [19],  $\gamma = 1 + (R_u T \Gamma_\infty / \gamma_s) \log(1 - \Gamma)$ , where  $\Gamma_\infty$  is the maximum surfactant concentration on the interface.  $T$  is the temperature and  $R_u$  is the universal gas constant. Eq. (31) can be written as

$$\sigma_{rz} = -Ma \left( \frac{1}{1 - \Gamma} \right) \frac{\partial\Gamma}{\partial\rho}, \quad (32)$$

where  $Ma = \frac{R_u T \Gamma_\infty}{\epsilon^{1/2} \mu U_s}$  is the Marangoni number. For *Tetrahymena* in an aqueous solution of Tween 20 with concentrations 0.004-0.08 mol/m<sup>3</sup> as used in [7],  $Ma \sim O(10^4)$  where  $R_u = 8.314$  J/(mol·K),  $T \sim 298$  K,  $\Gamma_\infty \sim 3.53 \times 10^{-6}$  mol/m<sup>2</sup>,  $\epsilon = 0.1$  [20]. This means that a tiny change in the surfactant concentration leads to a large variation in the shear stress at the interface.

The leading order effect of the surfactant concentration leads to immobilization of the interface and invalidates the “perfect-slip” boundary condition. Guided by Eq. (32), the surfactant concentration  $\Gamma$  can be perturbed in terms of  $Ma^{-1}$  as

$$\Gamma = \Gamma_0 + Ma^{-1}\Gamma_1 + O(Ma^{-2}), \quad (33)$$

where  $\Gamma_0$  is a constant. The transport of surfactant is governed by a convection diffusion equation. The convection diffusion equation for the leading order term,  $\Gamma_0$ , simplifies to a pure convection equation  $\nabla_s \cdot (\mathbf{u}\Gamma_0) = 0$  on the interface [19]. The solution to this equation,  $u_\rho \Gamma = A/\rho$ , has to be bounded as  $\rho \rightarrow 0$ ; thus, the constant  $A = 0$ . Therefore,  $u_\rho = 0$  which

means that the leading order effect of the surfactant in a large Marangoni number limit is to immobilize the interface. For an immobilized interface (rigid wall), the pressure in the lubrication region is known [13]

$$p = \epsilon^{-3/2} \left( -\frac{6\rho}{5H_1} \sum_{n=1}^{\infty} B_n W_n \right) (\mathbf{e} \cdot \mathbf{e}_\rho), \quad (34)$$

and is in the order of  $O(\epsilon^{-3/2})$ , while the pressure is in the order of  $O(\epsilon^{-1})$  for a clean interface.

## V. CONCLUSION

Ciliate protozoa have been shown to be present in large concentrations in the neuston layer of both marine and freshwater ecosystems compared to bulk water [21, 22]. In this paper, we have considered the motion of a model ciliate swimming near an air-liquid interface. By satisfying the “perfect-slip” boundary condition, the lubrication theory is utilized to solve the flow field in the gap region. It is found that the pressure in the gap region is an important factor in determining the swimmer’s velocity perpendicular to the interface. The vertical swimming velocity is in the order of  $O(\epsilon \log \epsilon)$  and is reduced significantly compared to the vertical swimming velocity of a swimmer in an unbounded domain. This reduced velocity leads to a long residence time of the model ciliate near an air-liquid interface and consequently the formation of large aggregates of ciliates.

The pressure field for a swimmer near a flat interface and a rigid wall are dramatically different; the first non-zero term for the latter case is of order  $O(\epsilon^{-3/2})$  instead of  $O(\epsilon^{-1})$ . The case of a squirmer moving near a rigid wall has been studied in [13] and here we have summarized their results and highlighted the differences between squirmer near a wall and air-liquid interface. According to [13] a squirmer near a rigid wall generates force and torque given as

$$F_x^s \sim O(\log \epsilon), \quad T_y^s \sim O(\log \epsilon), \quad F_z^s \sim O(\log \epsilon). \quad (35)$$

The dimensionless force  $F_x$  and torque  $T_y$  acting on a particle translating with velocity  $U$  parallel to a wall can be written as

$$F_x \sim 6\pi \left( \frac{8}{15} \log \epsilon \right), \quad T_y \sim 8\pi \left( -\frac{1}{10} \log \epsilon \right). \quad (36)$$

The dimensionless force and torque acting on a sphere with angular velocity  $\Omega$  near a wall are

$$F_x \sim \frac{8\pi a\Omega}{U} \left( -\frac{1}{10} \log \epsilon \right), T_y \sim \frac{8\pi a\Omega}{U} \left( \frac{2}{5} \log \epsilon \right), \quad (37)$$

and finally, the force acting on a sphere moving perpendicular to a wall is  $F_z \sim -6\pi\epsilon^{-1}$ . Consequently, the translational velocity along the horizontal direction and angular velocity of a squirmer moving near a rigid wall are in the order  $U_x \sim O(1)$ ,  $\Omega \sim O(1)$ , while its vertical velocity is in the order of  $U_z \sim O(\epsilon \log \epsilon)$ .

The vertical velocity of a squirmer near both a rigid wall and air-liquid interface scale as  $\epsilon \log \epsilon$ . For the rigid wall, the leading order pressure scales as  $\epsilon^{-3/2}$  and for the air-liquid interface as  $\epsilon^{-1}$ . The horizontal force and torque in the lubrication region of a squirmer near a rigid wall dominate the force and torque calculated outside the lubrication region and scales as  $\log \epsilon$  but this is not the case for a squirmer moving near an air-liquid interface.

## ACKNOWLEDGMENTS

This work is supported by NSF grant CBET-1150348.

## Appendix

In order to calculate the forces and torque acting on the squirmer, we need to calculate the velocity field. The expression for the velocity field in terms of cylindrical coordinates  $(\rho, \phi, Z)$  are given below,

$$\begin{aligned} u_{\rho,1} &= \frac{Z^2 - H_1^2}{2} \left[ (\mathbf{e}_1 \cdot \mathbf{e}_\rho) \left( -\frac{3B}{5H_1^2} + \frac{6B\rho^2}{5H_1^3} \right) + C \left( -\frac{3\rho}{2H_1^2} - \frac{3\rho}{2H_1^3} \right) \right] \\ &\quad - \rho \left( (\mathbf{e}_1 \cdot \mathbf{e}_\rho)^2 \sum_{n=1}^{\infty} B_n W'_n + e_{13} \sum_{n=1}^{\infty} B_n W_n \right), \\ u_{\phi,1} &= (\mathbf{e}_\phi \cdot \mathbf{e}_1) (Z^2 - H_1^2) \left( -\frac{3B}{10H_1^2} \right) - (\mathbf{e}_\phi \cdot \mathbf{e}_1) (\mathbf{e}_\rho \cdot \mathbf{e}_1) \rho \sum_{n=1}^{\infty} B_n W'_n, \\ u_{z,1} &= (\mathbf{e}_\rho \cdot \mathbf{e}_1) \left[ \left( \frac{9B\rho}{5H_1} - \frac{3B\rho^3}{5H_1^2} \right) Z - \left( \frac{4B\rho}{5H_1^3} - \frac{3B\rho^3}{5H_1^4} \right) Z^3 \right] \\ &\quad + \left[ \left( -1 + \frac{3\rho^2}{4H_1} + \frac{3\rho^2}{4H_1^2} \right) CZ - \left( -\frac{1}{H_1^2} + \frac{3\rho^2}{4H_1^3} + \frac{3\rho^2}{4H_1^4} \right) CZ^3 \right]. \end{aligned} \quad (\text{A.1})$$

The force elements  $dF_\rho$ ,  $dF_z$ , and the torque element  $dT_y$  acting on the squirmer can be calculated as follows

$$\begin{aligned}
dF_z &= \mathbf{e}_z \cdot (\boldsymbol{\sigma} \cdot \mathbf{n})dA, \\
dF_x &= \mathbf{e}_x \cdot (\boldsymbol{\sigma} \cdot \mathbf{n})dA, \\
dT_y &= -\mathbf{n} \cdot \mathbf{e}_x dF_z + \mathbf{n} \cdot \mathbf{e}_z dF_x.
\end{aligned} \tag{A.2}$$

Using above equations, all the components of force and torque can be evaluated.  $F_z$  is given in Eq. (25) and  $F_x$  and  $T_y$  are given as follows:

$$\begin{aligned}
T_y &\sim \pi e_{11} B \int_\theta \left[ -3 \frac{\rho}{H_1} + \frac{24\rho^3}{5H_1^2} \right] \cos \theta \sin^2 \theta d\theta \\
&\quad + \pi e_{11} B \int_\theta \left[ \epsilon^{-1/2} \left( -\frac{6}{5H_1} + \frac{6\rho^2}{5H_1^2} \right) + \epsilon^{1/2} \left( 2 + \frac{3\rho^2}{5H_1} - \frac{6\rho^4}{5H_1^2} \right) \right] \cos^2 \theta \sin \theta d\theta \\
&\sim O(\epsilon^{1/2} \log \epsilon),
\end{aligned} \tag{A.3}$$

$$\begin{aligned}
F_x &\sim \frac{6}{5} \pi B e_{11} \int_\theta \left[ \left( \epsilon^{-1} \frac{\rho}{2H_1^2} \right) \sin^2 \theta - \left( -\frac{1}{H_1} + \frac{\rho^2}{H_1^2} \right) \epsilon^{-1/2} \cos \theta \sin \theta \right] d\theta \\
&\quad + \pi B e_{11} \int_\theta \left[ \left( \frac{9\rho}{5H_1} - \frac{12\rho^3}{5H_1^2} \right) \sin^2 \theta - \epsilon^{1/2} \left( 2 + \frac{3\rho^2}{5H_1} - \frac{6\rho^4}{5H_1^2} \right) \sin \theta \cos \theta \right] d\theta \\
&\sim O(\epsilon^{1/2} \log \epsilon).
\end{aligned} \tag{A.4}$$

- 
- [1] R. Trouilloud, T. S. Yu, A. E. Hosoi, and E. Lauga, *Phys. Rev. Lett.* **101**, 048102 (2008).
  - [2] R. Di Leonardo, L. Angelani, D. Dell’Arciprete, G. Ruocco, V. Iebba, S. Schippa, M. P. Conte, F. Mecarini, F. De Angelis, and E. Di Fabrizio, *Proc. Natl. Acad. Sci. U.S.A.* (2010).
  - [3] M. I. Gladyshev, *Biophysics of the Surface Microlayer of Aquatic Ecosystems* (IWA Publishing, London, 2002).
  - [4] R. Di Leonardo, D. Dell’Arciprete, L. Angelani, and V. Iebba, *Phys. Rev. Lett.* **106**, 038101 (2011).
  - [5] E. Naumann, *Biologisches Zentralblatt* **37**, 98106 (1917).
  - [6] J. S. Maki, *Neuston Microbiology: Life at the Air-water Interface* (John Wiley & Sons, Inc., 2003).

- [7] J. Ferracci, T. Ishikawa, H. Ueno, K. Numayamma, Y. Imai, and T. Yamaguchi, Nano-biomedical engineering 2012; proceedings of the Tohoku University Global Centre of Excellence Programme , 70 (2012).
- [8] S. E. Spagnolie and E. Lauga, *J. Fluid Mech.* **700**, 105 (2012).
- [9] S. H. Lee, R. S. Chadwick, and L. G. Leal, *J. Fluid Mech.* **93**, 705 (1979).
- [10] J. R. Blake, *J. Fluid Mech.* **46**, 199 (1971).
- [11] M. J. Lighthill, *Commun. Pur. Appl. Math.* **5** (1952).
- [12] K. Drescher, K. C. Leptos, I. Tuval, T. Ishikawa, T. J. Pedley, and R. E. Goldstein, *Phys. Rev. Lett.* **102**, 168101 (2009).
- [13] T. Ishikawa, M. P. Simmonds, and T. J. Pedley, *J. Fluid Mech.* **568**, 119 (2006).
- [14] D. Jeffery and R. Cordless, *PhysicoChem. Hydrodyn.* **10**, 461 (1988).
- [15] S. Kim and S. J. Karrila, *Microhydrodynamics: Principles and Selected Applications* (Courier Dover Publications, 1992) Chap. 9, pp. 219–238.
- [16] S. Wang and A. Ardekani, *Physics of Fluids* **24**, 101902 (2012).
- [17] T. J. Pedley and J. O. Kessler, *Annu. Rev. Fluid Mech.* **24**, 313 (1992).
- [18] R. N. Roslan, N. M. Hanif, M. R. Othman, W. N. F. W. Azmi, X. X. Yan, M. M. Ali, C. A. R. Mohamed, and M. T. Latif, *Marine Poll. Bull.* **60**, 1584 (2010).
- [19] L. Leal, *Advanced Transport Phenomena* (Cambridge University Press, 2007) Chap. 2, pp. 89–96.
- [20] P. Ghosh, *Colloid and Interface Science* (Phi Learning, 2009) Chap. 6, pp. 204–210.
- [21] W. D. Taylor and J. Berger, *Microb. Ecol.* **6**, 27 (1980).
- [22] N. Ricci, F. Erra, A. Russo, and R. Banchetti, *Limnol. Oceanogr.* **36**, 1178 (1991).